How to cite: *Angew. Chem. Int. Ed.* **2023**, *62*, e202313502
doi.org/10.1002/anie.202313502

Polymer Recycling

Metamorphosis of a Commodity Plastic like PVC to Efficient Catalytic Single-Chain Nanoparticles

*Agustín Blazquez-Martín, Ester Verde-Sesto, Arantxa Arbe, and José A. Pomposo**

Abstract: We perform the conversion of a commodity plastic of common use in pipes, window frames, medical devices, flexible hoses, etc. like polyvinyl chloride (PVC) to single-chain nanoparticles (SCNPs). SCNPs are versatile, protein-mimetic soft nano-objects of growing interest for catalysis, sensing, and nanomedicine, among other uses. We demonstrate that the metamorphosis process -as induced through metal-free click chemistry- leads to well-defined, uniform SCNPs that are stable during storage in the solid state for months. All the conversion process (from PVC isolation to PVC-SCNPs synthesis) can be run in a green, dipolar aprotic solvent and involving, when required, a simple mixture of ethanol and water (1/1 vol.) as non-solvent. The resulting PVC-SCNPs are investigated as recyclable, metalloenzyme-mimetic catalysts for several representative Cu(II)-catalyzed organic reactions. The method could be valid for the metamorphosis and valorization of other commodity plastics in which it is feasible to install azide functional groups in their linear polymer chains.

Introduction

In addition to recycling, waste valorization by converting polymeric waste materials into more useful products is attracting significant interest to mitigate plastic pollution issues. Polyvinyl chloride (PVC) is the 3rd most widely produced synthetic polymer in the world after the most commonly used polyolefins, polyethylene (PE) and polypropylene (PP).[1] Current global PVC production is estimated at ca. 40 million metric tonnes (Mt) per year. Around 6.5 Mt of PVC are annually manufactured in the European Union (EU) with ca. 2 Mt of post-consumer PVC waste generated.[2] Mechanical recycling of rigid PVC from the construction and building sector (e.g., windows, pipes) is currently the main relevant recycling process in the EU for post-consumer PVC waste. Recycling or valorization of flexible PVC waste from e.g. packaging, automotive and medical sectors is complicated by the difficulty to handle banned plasticizers (e.g., *bis*(2-ethylhexyl) phthalate) -still entering recycling streams- after isolation of neat PVC from flexible PVC waste. This seems to be the main cause of the closure in 2018 of the only plant in the EU established to recycle up to 10000 t of flexible PVC waste a year.[3] Incineration and landfilling represent the main non-recycling treatment routes for PVC.[2] Currently, significant effort is devoted by many research groups on breaking PVC down to useful products. For instance, Jin, Yoshioka et al. introduced a new and green approach to achieve—in a single step—the complete dechlorination of PVC, as well the conversion of hydrogen carbonate to formate with nearly 100 % selectivity and 16 % yield.[4] Sun, Xie and co-workers have recently reported the first highly selective conversion of PVC waste into C_2 fuels by a universal photoinduced sequential C–C bond cleavage and coupling pathway under simulated natural environment conditions.[5] Tour et al. were able to convert a mixture of plastic wastes containing PVC into flash graphene via flash Joule heating.[6] Additionally, Yoshioka et al. have developed the Cl recovery process,[7] which entails the dechlorination of PVC in NaOH/ethylene glycol (EG) solvent by ball-milling and treating the Cl ion dissolved in EG by electro-dialysis for the simultaneous recovery of NaCl and EG.

Herein, a complementary concept of polymeric waste valorization is introduced through metamorphosis of a commodity plastic like PVC to efficient catalytic single-chain nanoparticles (SCNPs). Synthetic SCNPs are obtained through folding/collapse of discrete functionalized polymer chains by means of intra-chain (reversible/covalent) interactions.[8] Within the local compact domains of SCNPs active species like catalysts, drugs, or luminophores can be immobilized either reversibly or permanently.[9] These soft nanoparticles open a plethora of opportunities for the development of new drug delivery vehicles, highly efficient catalysts and improved sensing elements, among other ones.[10] For instance, Paulusse

[*] A. Blazquez-Martín, Dr. E. Verde-Sesto, Prof. A. Arbe, Prof. J. A. Pomposo
Centro de Física de Materiales (CSIC—UPV/EHU)—Materials Physics Center MPC, P° Manuel de Lardizabal 5, E-20018 Donostia (Spain)
E-mail: josetxo.pomposo@ehu.eus
Dr. E. Verde-Sesto, Prof. J. A. Pomposo
IKERBASQUE—Basque Foundation for Science, Plaza Euskadi 5, E-48009 Bilbao (Spain)
Prof. J. A. Pomposo
Departamento de Polímeros y Materiales Avanzados: Física, Química y Tecnología. University of the Basque Country (UPV/EHU), PO Box 1072, E-20800 Donostia (Spain)

et al. developed a method for intracellular location of SCNPs by controlled surface modification with tertiary amines to improve intracellular targeting for biomedical applications.[11] Cheng et al. synthesized SCNPs loaded with the anticancer drug doxorubicin displaying selective cytotoxicity toward HeLa cancer cells, without affecting healthy NIH/3T3 cells.[12] Tang et al. showed polydopamine-coated surfaces containing SCNPs with excellent in vitro bactericidal activity against both *Staphylococcus aureus* and *Escherichia coli* with >99.9 % killing efficacy, excellent protein adsorption resistance, antibacterial adhesion and low cytotoxicity.[13] Recently, Yan et al. reported CO_2-folded SCNPs as recyclable, improved carboxylase mimics able to catalyze CO_2-insertion of C(sp^3)–H and, even, C(sp^2 and sp)–H substrates at room temperature (r.t.).[14] Additionally, Tan et al. synthesized enzyme-mimetic SCNPs containing chiral Fe(II)-oxazoline complexes allowing efficient asymmetric sulfa-Michael addition of thiols to a wide range α,β-unsaturated ketones in water at r.t. without the need of any organic solvent or additional additives.[15] Remarkably, Collot et al. reported stealth and bright monomolecular fluorescent SCNPs as artificial analogues of fluorescent proteins, surpassing the latter >50-fold in terms of brightness.[16] More recently, a strategy for self-reporting both intra-molecular compaction and inter-molecular aggregation of SCNPs based on the installation of orthogonal luminophores via Hantzsch ester formation has been developed by our group.[17] However, SCNPs have always been synthesized from specialty polymeric precursors, and not from waste of commodity plastics.

As illustrated in Scheme 1, we propose the metamorphosis of "PVC waste" to PVC-SCNPs in two steps: i) partial azidation of discrete linear PVC chains via nucleophilic substitution to give PVC-N_3 in which some of the chlorine atoms are replaced by azide groups; and ii) intra-chain reaction of individual PVC-N_3 chains with the Sondheimer diyne[18] (5,6,11,12-tetradehydro- dibenzo-[*a,e*]cyclooctene, **1**) via metal-free Huisgen cycloaddition reaction at r.t. to produce PVC-SCNPs. Two constraints of the valorization strategy reported in this work to produce PVC-SCNPs should be mentioned: the requirement of using PVC waste free from banned plasticizers, and the relatively expensive cost of **1**. The resulting PVC-SCNPs will be investigated as recyclable, metalloenzyme-mimetic catalysts.

Results and Discussion

As a proof-of-concept, we initially started by performing the metamorphosis process using neat, commercial PVC and common (non-green) organic solvents. PVC chains can be functionalized by nucleophilic substitution of the chlorine atoms with a range of nucleophiles (e.g., azide, thiolates, thiocyanate) through a S_N2 mechanism.[19] We target partial azidation of PVC to give PVC-N_3[20] as the right functionalization step for the subsequent intra-chain metal-free click chemistry procedure. In this sense, SCNPs are typically prepared from precursors containing between 10 and 30 mol % of functional groups.[8] It is well known that the degree of substitution in PVC depends on the nature of the nucleophile, the polarity of the solvent, temperature,and the duration of the reaction. We obtained a degree of substitution of 12.2 mol % by performing the azidation reaction with sodium azide (NaN_3, 1 equiv) in *N*,*N*-dimethylformamide (DMF) at 80 °C for 4 h, as revealed by elemental analysis (EA) data of PVC-N_3 after its isolation by precipitation in a

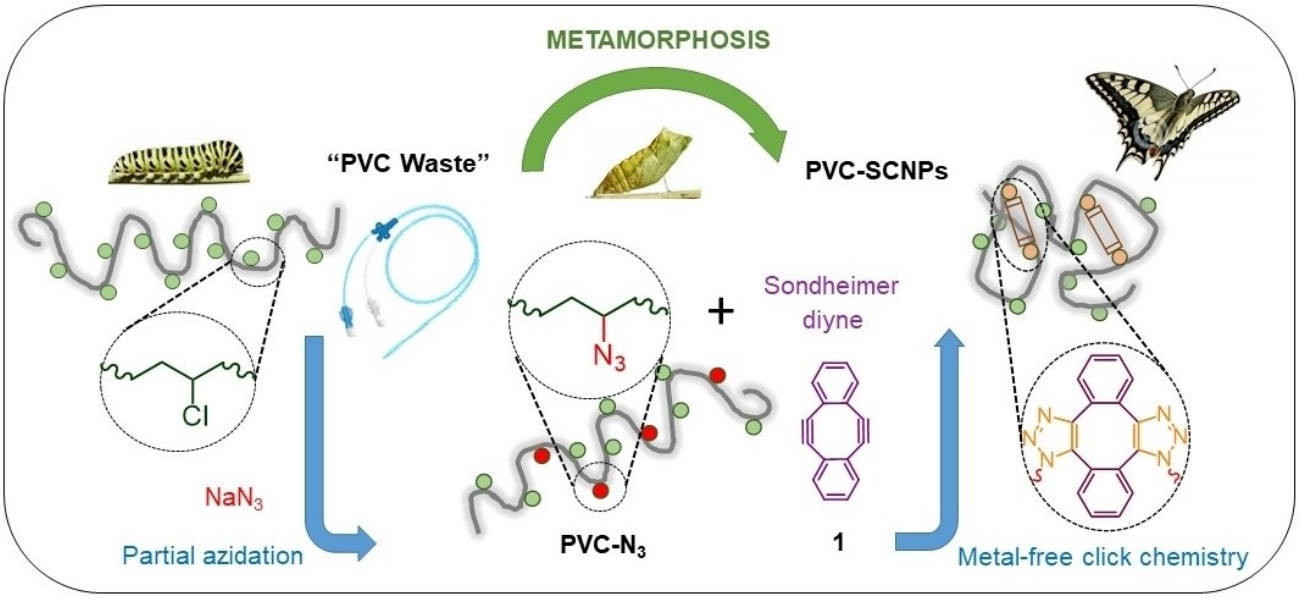

Scheme 1. Metamorphosis of "PVC waste" to PVC single-chain nanoparticles (PVC-SCNPs) in two steps: i) partial azidation of PVC to PVC-N_3; and ii) intra-chain metal-free click chemistry at r.t. involving individual PVC-N_3 chains and the Sondheimer diyne (5,6,11,12-tetradehydrodibenzo-[*a,e*]cyclooctene, **1**) to give PVC-SCNPs.

mixture of methanol (MeOH) and H_2O (1/1 vol.) followed by drying at 50 °C under vacuum for 24 h. These reaction conditions were selected to minimize secondary reactions that lead to aggregation during PVC-SCNP synthesis (see below). PVC-N_3 was subsequently characterized by proton (^{1}H) and carbon (^{13}C) nuclear magnetic resonance (NMR) spectroscopy, size exclusion chromatography (SEC) and infra-red (IR) spectroscopy (see Figure 1).

The ^{1}H NMR spectrum of commercial PVC (weight average molecular weight, $M_{w(MALLS)}$ = 46.5 kDa; dispersity, $Đ$ = 1.35) shows tacticity features in both the methine (Cl–C***H***–CH_2–) and methylene (Cl–CH–C***H₂***–) protons placed at 4.06–4.60 and 1.85–2.39 ppm, respectively.[20] Upon partial azidation, new bands appear in the ^{1}H NMR spectrum of PVC-N_3 located at 4.05–4.18 and 1.85 ppm that can be attributed, respectively, to N_3–C***H***–CH_2– methine and N_3–CH–C***H₂***– methylene protons (Figure 1a). Similarly, in the ^{13}C NMR spectrum of PVC-N_3 new signals from N_3–***C***H–CH_2– methine and N_3–CH–***C***H_2– methylene carbons are clearly visible at 55.8 and 42.0 – 43.3 ppm, respectively, when compared to the signals of neat PVC (Figure 1b). The weight average molecular weight and dispersity of PVC-N_3 ($M_{w(MALLS)}$ = 51.4 kDa, $Đ$ = 1.35) were found to be very similar to those of the starting PVC material, as determined by SEC (Figure 1c). Complementary, the IR spectrum of PVC-N_3 showed an intense band centered at ca. 2110 cm^{-1} corresponding to the stretching vibration of the azide moiety (Figure 1d). Taken together, these results support the successful (partial) functionalization of PVC chains in DMF with a number of azide pendants.

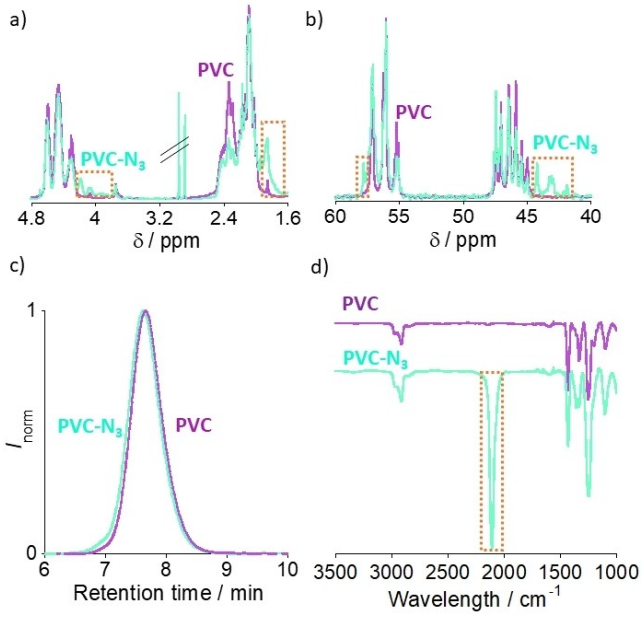

Figure 1. a) ^{1}H NMR spectra, b) ^{13}C NMR spectra, c) SEC traces (multi-angle laser-light scattering (MALLS) detector, THF, 1 mL min^{-1}) and d) IR spectra of PVC (purple) and PVC-N_3 (light green). New bands associated to PVC-N_3 after azidation of commercial PVC are highlighted by dotted orange squares.

As a next step towards SCNPs from PVC-N_3 we selected the strain-promoted double-click (SPDC) reaction as first introducedby Kii et al. for the chemical modification of azido-biomolecules,[21] by involving the Sondheimer diyne[18] (**1**, see Scheme 1) which is currently commercially available. **1** is a bisreactive molecule with two highly strained alkyne bonds ready to react spontaneously with two azide moieties of the same PVC-N_3 chain if the reaction is carried out at high dilution (i.e., below the critical overlap concentration of polymer coils, c^*).[8] Notably, the second cycloaddition reaction of **1** was predicted by a density functional theory method, and confirmed experimentally with model compounds, to have a lower activation energy (i.e., faster kinetics) than the first one due to the resulting highly-distorted alkyne bond.[22] Consequently, we expect a relatively fast intra-chain reaction of the second alkyne bond of **1** after the first cycloaddition of **1** and an azide group of a PVC-N_3 chain. It is worth of mention that in the case of polymer chains some differences from the reactivity of model compounds are expected due to conformational restrictions.[8] Nevertheless, due to the expected increased kinetics of the second cycloaddition reaction it its especially important to guarantee that no other PVC-N_3 chains are in close proximity. This requirement is only fulfilled by working at very high dilution conditions where the PVC-N_3 chains are truly isolated one from another. Trying to minimize as much as possible inter-chain coupling events, we carried out the intra-chain SPDC reaction of **1** within individual PVC-N_3 chains by means of a continuous addition technique[23] with tetrahydrofuran (THF) as the solvent. Hence, we feed slowly with a syringe pump (2.1 mL h^{-1}) a concentrated PVC-N_3 solution (2 mg mL^{-1}) into a diluted solution of **1** (0.2 mg mL^{-1}) under stirring, both solutions at r.t. (see Electronic Supporting Information, ESI, Figure S1). After optimization of the reaction conditions, we selected a molar ratio of alkyne (**1**) to azide (PVC-N_3) groups of 1.35. After complete addition of the PVC-N_3 solution (ca. 12 h), we left the system under stirring for additional 12 h to allow the strain-promoted double-click reaction to proceed until completion. Next, since we employed a small excess of **1** when compared to the amount of reactive azide groups in PVC-N_3, we added an appropriate amount of benzyl azide (see ESI) to deactivate any potentially unreacted strained alkyne bonds. Notably, this end-capping procedure was found to be essential to guarantee an excellent long-term stability of the resulting PVC-SCNPs (see below). We isolated the PVC-SCNPs by precipitation in cold ethanol (EtOH) to remove potential traces of low molecular weight compounds followed by further drying under vacuum at 50 °C.

Figure 2 shows the ^{1}H and ^{13}C NMR spectra of the PVC-SCNPs. The most notorious features are the presence of new bands in the ^{1}H and ^{13}C NMR spectra of the PVC-SCNPs coming from the incorporation of the intra-chain cross-linker **1** and the disappearance of the bands from N_3–C***H***–CH_2– and N_3–CH–C***H₂***– protons as well as N_3–***C***H–CH_2– and N_3–CH–***C***H_2– carbons when com-

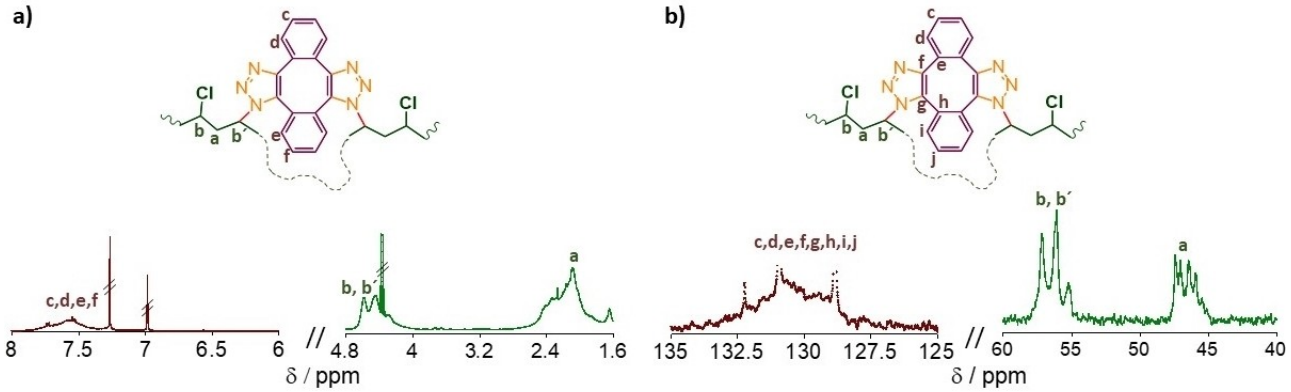

Figure 2. Selected regions of the a) ^{1}H NMR and b) ^{13}C NMR spectra of PVC-SCNPs synthesized via intra-chain metal-free click chemistry at r.t. from individual PVC-N_3 chains and the Sondheimer diyne (**1**) showing signals from protons and carbons of the main chain in green, and signals from protons and carbons of the intra-chain cross-linker in purple.

pared, respectively, to the ^{1}H and ^{13}C NMR spectra of PVC-N_3 (Figure 1a, b). SEC provided a solid confirmation of efficient formation of PVC-SCNPs. A shift towards longer SEC retention time and, hence, a reduction in average hydrodynamic size was clearly observed upon PVC-SCNPs formation (Figure 3a and Figure S2). Simultaneously, the weight average molecular weight and dispersity of PVC-SCNPs ($M_{w(MALLS)} = 92.1$ kDa, $Đ = 1.34$) were consistent with the expected behavior upon incorporation of **1** as intra-chain cross-linker. Dynamic light scattering (DLS) measurements in THF (Figure 3b) confirmed a reduction in average hydrodynamic radius from 10.1 nm (PVC-N_3) to 6.5 nm (PVC-SCNPs). Complementarily, we determined the radius of gyration (R_g) and size-scaling exponent (ν) of PVC-N_3 and PVC-SCNPs by means of small-angle X-ray scattering (SAXS) measurements (see ESI). PVC-N_3 showed $R_{g(PVC\text{-}N3)} = 14.7$ nm and $\nu_{(PVC\text{-}N3)} \approx 0.6$ -the typical value for linear polymer chains in good solvent conditions- (Figure S3). As expected, PVC-SCNPs showed a significant reduction in both R_g and ν: $R_{g(PVC\text{-}SCNPs)} = 6.7$ nm, $\nu_{(PVC\text{-}SCNPs)} = 0.46$ (Figure S4). A reduction in R_g and ν is commonly observed upon intra-chain folding of isolated chains to produce SCNPs.[8,17] Specifically, the lower value of ν in the case of PVC-SCNPs when compared to $\nu_{(PVC\text{-}N3)} \approx 0.6$ is a clear indication of a higher level of chain compaction. More importantly, no significant changes were detected when the PVC-SCNPs were subjected to SAXS experiments after 2 months of storage in the solid state (Figure 3 and Figure S5), or when stored in THF solution for 2 months (Figure S6). These experimental findings show that the PVC-SCNPs are highly stable during storage and no significant inter-chain aggregation processes were involved either in solution or in the solid state for months. We attribute this stability to the final end-capping procedure with benzyl azide that is able to limit the number of residual reactive functional groups. Also, the absence of any metallic catalyst in the intra-chain cross-linking step contributes -presumably- to the stability of the PVC-SCNPs. Folding of individual PVC-N_3 chains to PVC-SCNPs resulted, additionally, in a modification of the thermal properties of the bulk material as illustrated in Figure 3d and Figure S7. Partial azidation of PVC to PVC-N_3 decreased by 10 °C the glass transition temperature (from $T_{g(PVC)} = 80$ °C to $T_{g(PVC\text{-}N3)} = 70$ °C) due to an increase in free volume introduced by the azide pendants, when compared to the chlorine moieties.[24] Interestingly, the glass transition temperature increased by 15 °C upon PVC-SCNPs formation ($T_{g(PVC\text{-}SCNPs)} = 85$ °C) as a consequence of the reduced segmental mobility caused by the

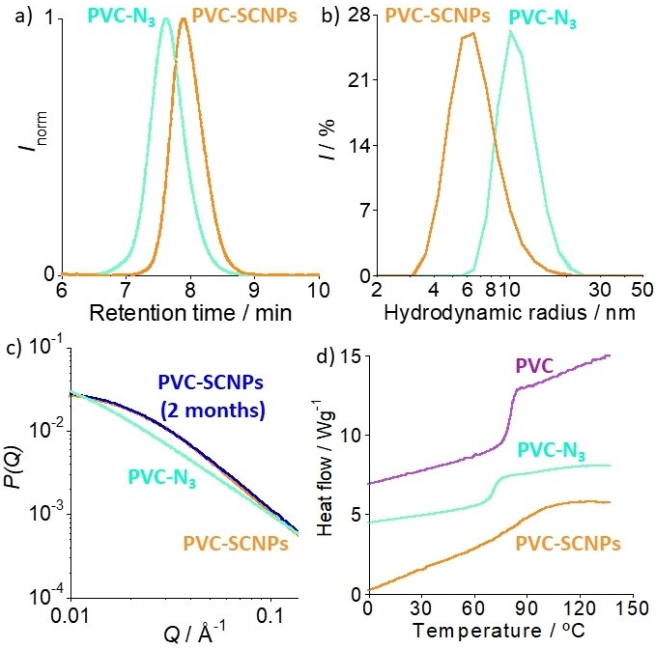

Figure 3. a) SEC traces (MALLS detector, THF, 1 mL min^{-1}) of PVC-N_3 (light green) and PVC-SCNPs (orange), b) DLS size distributions of PVC-N_3 (light green) and PVC-SCNPs (orange), c) SAXS results of PVC-N_3 (light green), PVC-SCNPs just after synthesis (orange) and after 2 months of storage in the solid state (blue), and d) DSC traces of neat PVC (purple), PVC-N_3 (light green) and PVC-SCNPs (orange). The PVC-N_3 and PVC-SCNPs traces have been downshifted for clarity.

intra-chain cross-links (Figure S8). All the above results support the successful formation of stable, well-defined PVC-SCNPs via intra-chain metal-free click chemistry at r.t. from commercial PVC and common organic solvents.

Next, we investigated if the same concept could be implemented for valorization of real "PVC waste" involving green and sustainable solvents[25] instead of DMF and THF, as well as EtOH and water as replacement for MeOH. Although we initially selected dihydrolevoglucosenone (Cyrene™) as a green, apolar diprotic solvent derived from waste cellulosic biomass, the PVC azidation step was found to require longer time and higher temperature in this non-mutagenic solvent than in DMF. Even worse, during PVC-SCNPs synthesis in this green solvent we systematically observed significant aggregation of the PVC-SCNPs (Figure S9). To solve this problem, we turned our attention to *N*-butylpyrrolidinone (NBP) (Figure 4a) as a non-reproductively toxic substance (according to OECD 414 test method), non-mutagenic compound (OECD 471) and inherently biodegradable (OECD 302B) dipolar aprotic solvent, which

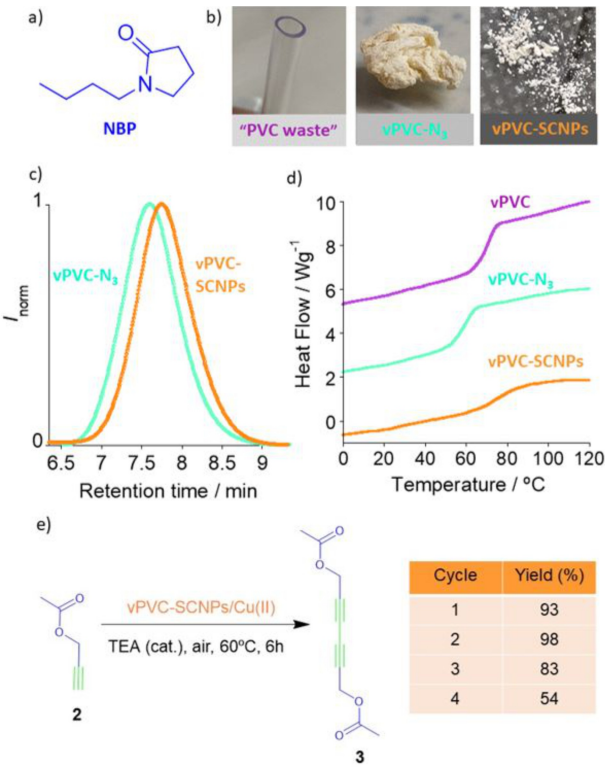

Figure 4. a) Chemical structure of *N*-butylpyrrolidinone (NBP) selected as alternative dipolar aprotic solvent to DMF. b) Metamorphosis of "PVC waste" to "valorized" PVC single-chain nanoparticles, vPVC-SCNPs, following the valorization process depicted in Scheme 1 using only NBP as "green" solvent, and a cold mixture of EtOH / H_2O (1/1 vol.) as non-solvent. c) SEC traces (MALLS detector, THF, 1 mL min^{-1}) of vPVC-N_3 (purple) and vPVC-SCNPs (orange). d) DSC traces of vPVC (purple), vPVC-N_3 (light green) and vPVC-SCNPs (orange). Traces of vPVC-N_3 and vPVC-SCNPs are downshifted for clarity. e) "Valorized" PVC single-chain nanoparticles loaded with 7.3 mol% of Cu(II) ions, denoted as vPVC-SCNPs/Cu(II), were employed as heterogeneous, recyclable catalyst in the homocoupling reaction of neat propargyl acetate (**2**) (TEA = triethylamine).

is commercially available in industrial relevant quantities (Solvagreen™, TamiSolve™).[26] Recently, NBP has been reported as the best green solvent candidate to replace reprotoxic DMF in solid-phase peptide synthesis.[27] We found that all the process comprising PVC isolation, PVC azidation and PVC-SCNPs synthesis can be efficiently carried out in NBP, using exactly the same reaction conditions during the azidation step as in DMF (80 °C, 4 h). Azidation of PVC in other green solvents under such conditions resulted in a significant lower azidation degree (see Figure S10).

We selected an out-of-use piece of clear flexible PVC hose (Figure 4b) for valorization to PVC-SCNPs, and we started by isolating the PVC material (valorized PVC, vPVC) by a solution/precipitation method using NBP as the solvent and a cold mixture of EtOH and water (1/1 vol.) as non-solvent. The dried vPVC ($M_{w(MALLS)}$ = 104.9 kDa, $Đ$ = 1.57) was subjected to azidation with NaN_3 (1 equiv) in NBP at 80 °C for 4 h, and isolated by precipitation in cold EtOH/H_2O (1/1 vol.) and further drying under vacuum at 50 °C. Successful partial azidation of vPVC in NBP to give vPVC-N_3 was confirmed by the same characterization techniques previously employed for the azidation of neat, commercial PVC. Specifically, the degree of chlorine substitution of vPVC in NBP was found to be 16.0 mol %, as determined by EA (Table S1). The stretching vibration of the azide moiety at ca. 2110 cm^{-1} was clearly visible in the IR spectrum of vPVC-N_3 (see Figure S11) whereas no relevant changes in both M_w and $Đ$ were found by SEC after azidation of vPVC in NBP (see ESI, Table S4). Figure 4c shows a comparison of the SEC traces of vPVC-N_3 and valorized PVC-SCNPs (vPVC-SCNPs) prepared using only NBP as green solvent, and a cold mixture of EtOH/H_2O (1/1 vol.) as non-solvent. vPVC-SCNPs showed a clear shift towards longer SEC retention time, as a consequence of reduced hydrodynamic size when compared to vPVC-N_3. Complementary, size reduction upon vPVC-SCNPs formation was also confirmed by DLS and SAXS measurements (see Figures S12–S14). Moreover, as illustrated in Figure 4d, the thermal behavior of vPVC, vPVC-N_3, and vPVC-SCNPs was almost identical to that recorded for PVC, PVC-N_3, and PVC-SCNPs (Figure 3d). Taken together, the above results confirm the successful metamorphosis of an out-of-use piece of clear flexible PVC hose to vPVC-SCNPs in "green" media involving only NBP, EtOH and H_2O. It is worth noting that the method also works for rigid PVC waste, so very similar results were obtained starting with a rigid PVC pipe (see ESI and Figure S15).

The locally compact domains of SCNPs offer a plethora of opportunities for the development of recyclable, enzyme-mimetic catalysts by using the beneficial outer coordination sphere effect of the folded/collapsed chain.[28] In this sense, we loaded the vPVC-SCNPs with Cu(II) ions (7.3 mol %) (see ESI) and investigated the resulting vPVC-SCNPs as recyclable / enzyme-mimetic catalysts for a variety of Cu(II)-catalyzed reactions.

First, we selected the solvent-free alkyne homocoupling reaction[29] as a benchmark transformation to investigate the efficiency and recyclability of the resulting vPVC-SCNPs/

Cu(II) (see Figure 4e and Figures S16–S21). We found that vPVC-SCNPs/Cu(II) when combined with neat propargyl acetate (PAc, **2**) and a catalytic amount of triethylamine (TEA) under air atmosphere for 6 h at 60 °C provided hexa-2,4-diyne-1,6-diyl diacetate (**3**) in very good yield (93 %). Interestingly, vPVC-SCNPs/Cu(II) can be easily recycled several times without losing catalytic activity (Figure 4e) and neither acidic nor thermal treatment was required, only filtration followed by drying under vacuum overnight. Consequently, the vPVC-SCNPs/Cu(II) catalyst offers a significant advantage over the homologous inorganic catalyst ($CuCl_2$) that showed 86 % yield in the first reaction cycle, but was found to be completely inactive when isolated following our conditions and used in a second homocoupling reaction of **2** (see ESI). We attribute the superior activity and recyclability of the vPVC-SCNPs/Cu(II) catalyst over $CuCl_2$ to both the confinement effect offered by the folded/collapsed nanoparticles to the Cu(II) ions and to the presence of triazole-Cu(II) interactions within the locally compact domains of the SCNPs. The decreased yield after three reaction cycles was a consequence of the progressive aggregation of the SCNPs, as revealed by DLS in combination with a leaching experiment (Figures S22–S24). Upon SCNPs aggregation, most of the active catalytic sites become inaccessible to the substrate. In this sense, vPVC-SCNPs/Cu(II) were found to be efficient catalysts for the homocoupling of polar alkynes (e.g., 1-ethynyl-4-fluorobenzene) but failed in the case of relatively apolar ones (e.g., 1-octyne) (see ESI, Figures S25–S26).

Next, we investigated the metalloenzyme-mimetic properties of vPVC-SCNPs/Cu(II) in the transformation of a *o*-diphenol model compound (3,5-di-*tert*-butylcatechol, DTBC) into a *o*-quinone product (3,5-di-tert-butyl-*o*-quinone, DTBQ) (see ESI). Reactions were carried out in a methanol/DMF (1/1 vol.) mixture in which the vPVC-SCNPs/Cu(II) catalyst was soluble. The successful formation of DTBQ was followed by UV/Vis spectroscopy (Figure 5a). As illustrated in Figure 5b, higher conversion and faster initial rate of reaction were observed for vPVC-SCNPs/Cu(II) when compared to $CuCl_2$ at identical Cu(II) concentration (Figure S27). At constant concentration of the vPVC-SCNPs/Cu(II) catalyst (Figure S28), a kinetic saturation pattern was found at high substrate concentration (Figure 5c) resembling enzyme-like behavior.[30] Analysis of the data in Figure 5c provided an apparent Michaelis–Menten constant ($K_{M,app}$) of 2.33 mM and an apparent catalytic constant ($k_{cat,app}$) of $1.98\times10^2\ h^{-1}$. Notably, the catalytic activity of vPVC-SCNPs/Cu(II) is similar to that reported for some model copper complexes of the catechol oxidase metalloenzyme,[31] as well as to the catalytic activity of aldolase enzyme-mimetic SCNPs reported by Huerta et al.[32] ($K_{M,app}=5.36$ mM, $k_{cat,app}=1.91\times10^2\ h^{-1}$).

Aditionally, we performed a comparison of the vPVC-SCNPs/Cu(II) catalyst against $CuCl_2$ for the oxidation reaction of styrene to benzaldehyde in the presence of hydrogen peroxide.[33] vPVC-SCNPs/Cu(II) in acetonitrile at 70 °C for 30 min provided benzaldehyde in 66 % yield, whereas the reaction yield dropped to 28 % with the homologous inorganic catalyst even at a higher concentration of Cu(II) in the latter case (see ESI, Figures S29–S30). The turnover frequency (moles of product per mole of catalyst per unit of time, TOF) of the vPVC-SCNPs/Cu(II) catalyst in this reaction was $4.9\times10^4\ h^{-1}$, higher than that reported for Cu(II)-triazole complexes (TOF = $1.2\times10^2\ h^{-1}$).[33] All the above results pave the way to the potential use of vPVC-SCNPs/Cu(II) as efficient catalyst in other Cu(II)-catalyzed organic transformations (e.g., cyclopropanation, Chan–Lam coupling, Henry reaction).

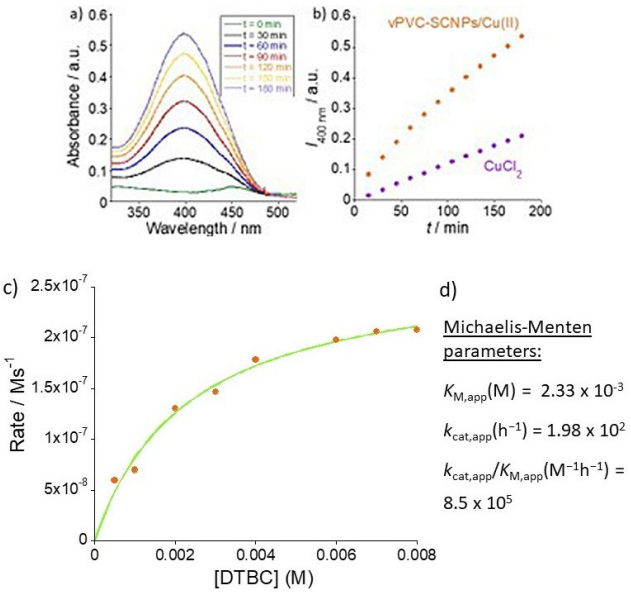

Figure 5. a) Characteristic UV absorption band of DTBQ at ca. 400 nm upon aerobic catalytic oxidation of DTBC over time using vPVC-SCNPs/Cu(II) as enzyme-mimetic catalyst. b) Illustration of the superior catalytic activity of vPVC-SCNPs/Cu(II) vs. $CuCl_2$ at identical Cu(II) concentration. c) Enzyme-like kinetics of vPVC-SCNPs/Cu(II) in the oxidation of DTBC to DTBQ. d) Michaelis–Menten kinetic parameters obtained from the data shown in c).

Conclusion

In conclusion, we disclose a complementary concept of polymeric waste valorization (upcycling) by metamorphosis of a commodity plastic of common use in daily life like polyvinyl chloride (PVC) to "valorized" PVC single-chain nanoparticles (vPVC-SCNPs). The full valorization process (PVC isolation, PVC azidation, vPVC-SCNPs synthesis) can be run in a green, dipolar aprotic solvent like NBP and involving, when required, a simple mixture of EtOH and H_2O (1/1 vol.) as non-solvent. We show that the metamorphosis process when carried out via metal-free click chemistry by means of the Sondheimer diyne as intra-chain cross-linker plus a specific end-capping procedure with benzyl azide leads to well-defined, uniform vPVC-SCNPs that are stable during storage in the solid state for months. We demonstrate that vPVC-SCNPs when loaded with 7.3 mol % of Cu(II) ions -to give vPVC-SCNPs/Cu(II)- become an efficient and recyclable catalyst in the solvent-free homocoupling reaction of polar

alkynes, showing enzyme-mimetic behavior in the oxidation of 3,5-di-*tert*-butylcatechol to 3,5-di-tert-butyl-*o*-quinone as well as very high TOF in the peroxidative oxidation of styrene to benzaldehyde. We envision the use of vPVC-SCNPs/Cu(II) as efficient catalyst in other Cu(II)-catalyzed organic transformations like cyclopropanation, Chan–Lam coupling or the Henry reaction, among other ones. Notably, this new concept is amenable for the valorization of other commodity plastics in which it is feasible to install azide functional groups along their linear polymer chains.

Acknowledgements

We gratefully acknowledge Grant PID2021-123438NB-I00 funded by MCIN/AEI/10.13039/501100011033 and "ERDF A way of making Europe", Grant TED2021-130107A-I00 funded by MCIN/AEI/10.13039/501100011033 and Unión Europea "NextGenerationEU/PRTR" and Grant IT-1566-22 from Eusko Jaurlaritza (Basque Government). We thank Amaia Iturrospe for technical support with SAXS experiments.

Conflict of Interest

The authors declare no conflict of interest.

Data Availability Statement

The data that support the findings of this study are available from the corresponding author upon reasonable request.

Keywords: Catalysis · Green Solvents · PVC Single-Chain Nanoparticles (SCNPs) · Polymeric Waste Valorization · Upcycling

[1] OECD, *Global Plastics Outlook: Economic Drivers, Environmental Impacts and Policy Options*, OECD Publishing, Paris, **2022**. https://doi.org/10.1787/de747aef-en.
[2] European Commission, Directorate-General for Environment, *The use of PVC (poly vinyl chloride) in the context of a non-toxic environment: final report*, **2022**. https://data.europa.eu/doi/10.2779/375357.
[3] J. Sherwood, *Johnson Matthey Technol. Rev.* **2020**, *64*, 4–15.
[4] L. Lu, H. Zhong, T. Wang, J. Wu, F. Jin, T. Yoshioka, *Green Chem.* **2020**, *22*, 352–358.
[5] X. Jiao, K. Zheng, Q. Chen, X. Li, Y. Li, W. Shao, J. Xu, J. Zhu, Y. Pan, Y. Sun, Y. Xie, *Angew. Chem. Int. Ed.* **2020**, *59*, 15497–15501.
[6] W. A. Algozeeb, P. E. Savas, D. X. Luong, W. Chen, C. Kittrell, M. Bhat, R. Shahsavari, J. M. Tour, *ACS Nano* **2020**, *14*, 15595–15604.
[7] a) J. Lu, S. Kumagai, Y. Fukushima, H. Ohno, S. Borjigin, T. Kameda, Y. Saito, T. Yoshioka, *ACS Sustainable Chem. Eng.* **2021**, *9*, 14112–14123; b) T. Kameda, H. Ohno, G. Grause, T. Mizoguchi, T. Yoshioka, *Ind. Eng. Chem. Res.* **2008**, *47*, 8619–8624; c) T. Kameda, S. Fukushima, C. Shoji, G. Grause, T. Yoshioka, *J. Mater. Cycles Waste Manage.* **2013**, *15*, 111–114.
[8] *Single-Chain Polymer Nanoparticles: Synthesis, Characterization, Simulations, and Applications* (Ed.: J. A. Pomposo), Wiley-VCH, Weinheim, **2017**.
[9] a) H. Frisch, B. T. Tuten, C. Barner-Kowollik, *Isr. J. Chem.* **2020**, *60*, 86–99; b) J. Chen, E. S. Garcia, S. C. Zimmerman, *Acc. Chem. Res.* **2020**, *53*, 1244–1256; c) R. Chen, E. B. Berda, *ACS Macro Lett.* **2020**, *9*, 1836–1843; d) E. Verde-Sesto, A. Arbe, A. Moreno, D. Cangialosi, A. Alegría, J. Colmenero, J. A. Pomposo, *Mater. Horiz.* **2020**, *7*, 2292–2313; e) G. M. ter Huurne, A. R. A. Palmans, E. W. Meijer, *CCS Chem.* **2019**, *1*, 64–82; f) S. Mavila, O. Eivgi, I. Berkovich, N. G. Lemcoff, *Chem. Rev.* **2016**, *116*, 878–961; g) C. K. Lyon, A. Prasher, A. M. Hanlon, B. T. Tuten, C. A. Tooley, P. G. Frank, E. B. Berda, *Polym. Chem.* **2015**, *6*, 181–197; h) M. Gonzalez-Burgos, A. Latorre-Sanchez, J. A. Pomposo, *Chem. Soc. Rev.* **2015**, *44*, 6122–6142.
[10] a) J. F. Hoffmann, A. H. Roos, F.-J. Schmitt, D. Hinderberger, W. H. Binder, *Angew. Chem. Int. Ed.* **2021**, *60*, 7820–7827; b) C. Stuckhardt, M. Wissing, A. Studer, *Angew. Chem. Int. Ed.* **2021**, *60*, 18605–18611; c) M. A. M. Alqarni, C. Waldron, G. Yilmaz, C. R. Becer, *Macromol. Rapid Commun.* **2021**, *42*, 2100035; d) M. H. Barbee, Z. M. Wright, B. P. Allen, H. F. Taylor, E. F. Patteson, A. S. Knight, *Macromolecules* **2021**, *54*, 3585–3612; e) E. S. Garcia, T. M. Xiong, A. Lifschitz, S. C. Zimmerman, *Polym. Chem.* **2021**, *12*, 6755–6760; f) S. Liao, L. Wei, L. A. Abriata, F. Stellacci, *Macromolecules* **2021**, *54*, 11459–11467; g) J. J. Piane, L. E. Chamberlain, S. Huss, L. T. Alameda, A. C. Hoover, E. Elacqua, *ACS Catal.* **2020**, *10*, 13251–13256; h) F. Eisenreich, E. W. Meijer, A. R. A. Palmans, *Chem. Eur. J.* **2020**, *26*, 10355–10361.
[11] N. M. Hamelmann, J.-W. D. Paats, J. M. J. Paulusse, *ACS Macro Lett.* **2021**, *10*, 1443–1449.
[12] C.-C. Cheng, S.-Y. Huang, W.-L. Fan, A.-W. Lee, C.-W. Chiu, D.-J. Lee, J.-Y. Lai, *ACS Appl. Polym. Mater.* **2021**, *3*, 474–484.
[13] X. Tian, R. Xue, F. Yang, L. Yin, S. Luan, H. Tang, *Biomacromolecules* **2021**, *22*, 4306–4315.
[14] R. Zeng, L. Chen, Q. Yan, *Angew. Chem. Int. Ed.* **2020**, *59*, 18418–18422.
[15] W. Wang, J. Wang, S. Li, C. Li, R. Tan, D. Yin, *Green Chem.* **2020**, *22*, 4645–4655.
[16] M. Collot, J. Schild, K. T. Fam, R. Bouchaala, A. S. Klymchenko, *ACS Nano* **2020**, *14*, 13924–13937.
[17] J. De–La-Cuesta, E. Verde-Sesto, A. Arbe, J. A. Pomposo, *Angew. Chem. Int. Ed.* **2021**, *60*, 3534–3539.
[18] H. N. C. Wong, P. J. Garratt, F. Sondheimer, *J. Am. Chem. Soc.* **1974**, *96*, 5604–5605.
[19] a) S. Marian, G. Levin, *J. Appl. Polym. Sci.* **1981**, *26*, 3295–3304; b) M. Takeishi, M. Okawara, *J. Polym. Sci. Part B* **1969**, *7*, 201–203.
[20] A. Earla, R. Braslau, *Macromol. Rapid Commun.* **2014**, *35*, 666–671.
[21] I. Kii, A. Shiraishi, T. Hiramatsu, T. Matsushita, H. Uekusa, S. Yoshida, M. Yamamoto, A. Kudo, M. Hagiwara, T. Hosoya, *Org. Biomol. Chem.* **2010**, *8*, 4051–4055.
[22] a) S. Yoshida, A. Shiraishi, K. Kanno, T. Matsushita, K. Johmoto, H. Uekusa, T. Hosoya, *Sci. Rep.* **2011**, *1*, 82; b) P. Sun, J. Chen, J. Liu, K. Zhang, *Macromolecules* **2017**, *50*, 1463–1472.
[23] E. Harth, B. V. Horn, V. Y. Lee, D. S. Germack, C. P. Gonzales, R. D. Miller, C. J. Hawker, *J. Am. Chem. Soc.* **2002**, *124*, 8653–8660.
[24] R. P. White, J. E. G. Lipson, *Macromolecules* **2016**, *49*, 3987–4007.
[25] A. Jordan, C. G. J. Hall, L. R. Thorp, H. F. Sneddon, *Chem. Rev.* **2022**, *122*, 6749–6794.

[26] J. Sherwood, H. L. Parker, K. Moonen, T. J. Farmera, A. J. Hunt, *Green Chem.* **2016**, *18*, 3990–3996.
[27] A. Kumar, M. Alhassan, J. Lopez, F. Albericio, B. G. de la Torre, *ChemSusChem* **2020**, *13*, 5288–5294.
[28] a) S. Thanneeru, J. K. Nganga, A. S. Amin, B. Liu, L. Jin, A. M. Angeles-Boza, J. He, *ChemCatChem* **2017**, *9*, 1157–1162; b) H. Rothfuss, N. D. Knöfel, P. W. Roesky, C. Barner-Kowollik, *J. Am. Chem. Soc.* **2018**, *140*, 5875–5881; c) J. Rubio-Cervilla, E. González, J. A. Pomposo, *Nanomaterials* **2017**, *7*, 341; d) C. A. Tooley, S. Pazicni, E. B. Berda, *Polym. Chem.* **2015**, *6*, 7646–7651.
[29] a) C. Glaser, *Liebigs Ann.* **1870**, *154*, 137–171; b) A. S. Hay, *J. Org. Chem.* **1962**, *27*, 3320–3321; c) D. Wang, J. Li, N. Li, T. Gao, S. Hou, B. Chen, *Green Chem.* **2010**, *12*, 45–48; d) P. Siemsen, R. C. Livingston, F. Diederich, *Angew. Chem. Int. Ed.* **2000**, *39*, 2632–2657.
[30] K. S. Banu, T. Chattopadhyay, A. Banerjee, S. Bhattacharya, E. Suresh, M. Nethaji, E. Zangrando, D. Das, *Inorg. Chem.* **2008**, *47*, 7083–7093.
[31] S. K. Dey, A. Mukherjee, *Coord. Chem. Rev.* **2016**, *310*, 80–115.
[32] E. Huerta, P. J. M. Stals, E. W. Meijer, A. R. A. Palmans, *Angew. Chem. Int. Ed.* **2013**, *52*, 2906–2910.
[33] Y. P. Petrenko, K. Piasta, D. M. Khomenko, R. O. Doroshchuk, S. Shova, G. Novitchi, Y. Toporivska, E. Gumienna-Kontecka, L. M. D. R. S. Martins, R. D. Lampeka, *RSC Adv.* **2021**, *11*, 23442–23449.

Manuscript received: September 11, 2023
Accepted manuscript online: October 4, 2023
Version of record online: October 12, 2023